Molecular Chain Movements and Transitions of SEBS above Room Temperature Studied by Moving-Window Two-Dimensional Correlation Infrared Spectroscopy

Tao Zhou,[†] Aiming Zhang,*[,†] Changsheng Zhao,[†] Hongwen Liang,[‡] Zhiyong Wu,[‡] and Jingkui Xia[‡]

The State Key Laboratory of Polymer Materials and Engineering of China, Polymer Research Institute, Sichuan University, Chengdu 610065, China; and Baling Petrochemical Industry Co., Ltd., of China Sinopec, Yueyang 414014, China

Received July 22, 2007; Revised Manuscript Received October 2, 2007

ABSTRACT: The temperature-dependent molecular chain movements and transitions of polystyrene-*block*-poly(ethylene-*co*-1-butene)-*block*-polystyrene block copolymer (SEBS) above room temperature were studied by in-site infrared spectroscopy combined with moving-window two-dimensional (MW2D) correlation spectroscopy. Some complex molecular chain movements and transitions of SEBS were revealed with the linear incremental temperature increasing (30−166 °C). The melting point of the extraordinary weak crystal of $-(CH_2-CH_2)-_n$ in the poly(ethylene-*co*-1-butene) block (EB) is determined at 48 °C. The heat enthalpy relaxation of polystyrene block (S) of SEBS, which is induced by the framework movement of the side benzene ring and the melting of the weak crystal in the polystyrene block, is observed around 72−80 °C from the MW2D correlation spectrum. The glass transition temperature of the polystyrene block is determined around 120 °C. From the MW2D correlation spectrum, we discover that, around 120 °C, the chain segment movement of polystyrene block occurs before that of poly(ethylene-*co*-1-butene) block in phase interface. At 142 °C, the fundamental chains of the disperse phase (S block) center initiate to entirely move and this type of movement drives a fraction of the disperse phase (S block) to deform from an incomplete shape to a sphere. This corresponds to the entirely viscous flow temperature of the fundamental chains of the disperse phase.

1. Introduction

Polystyrene-*block*-poly(ethylene-*co*-1-butene)-*block*-polystyrene block copolymer (SEBS) is one of the earliest used industrial and commercial thermoplastic elastomers.[1−3] So far SEBS has widespread availability in various areas, for example, daily necessities, toys, stamping steel ribbon, and medical instruments.[1] SEBS is synthesized using active anionic polymerization, where the three-step method is the most used.[4,5] Figure 1 illustrates the molecular structure of SEBS, which has polystyrene (hard block S) at both ends and poly(ethylene-*co*-1-butene) (soft block EB) in the middle. Because of the solubility parameter difference between polystyrene and poly(ethylene-*co*-1-butene) of SEBS, phase separation is its certain physical characteristics. Like other block copolymers, SEBS exhibits various and beautiful phase patterns with the S block (or EB block) volume ratio variation and other conditions changing;[1,6−16] however, in commercial SEBS, due to processability, as well as excellent mechanical properties, the hard block (S) is always disperse phase and the soft block (EB) is continuous phase (Figure 2). Generally speaking, in the process of SEBS synthesis, the soft block is always artificially introduced at 25−40 wt % by a 1,2-addition reaction (butadiene) before hydrogenising, and therefore in final commercial products the crystalline nature of $-(CH_2-CH_2)-_n$ of the soft block is effectively suppressed.[1] Consequently, SEBS is endowed with outstanding elastic behavior and transparency.

The temperature-dependent characteristics of SEBS was investigated by several researchers. According to the literature,[12−22] the experimental methods for these studies are based on small-angle X-ray (SAXS), small-angle neutron scattering (SANS), dynamic mechanical thermal analysis (DMTA), differential scanning calorimetry measurements (DSC), transmission electron microscopy (TEM), and atomic force microscopy (AFM). However, most of these studies on these systems are concerned with the microphase separation and morphology, the rheological

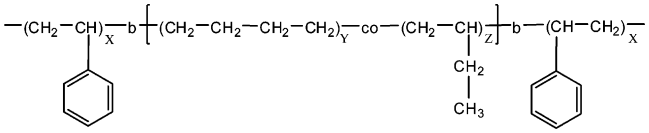

Figure 1. Molecular structure of SEBS. X and $Y + Z$ represent the polymerization degrees of the hard and soft blocks of SEBS, respectively.

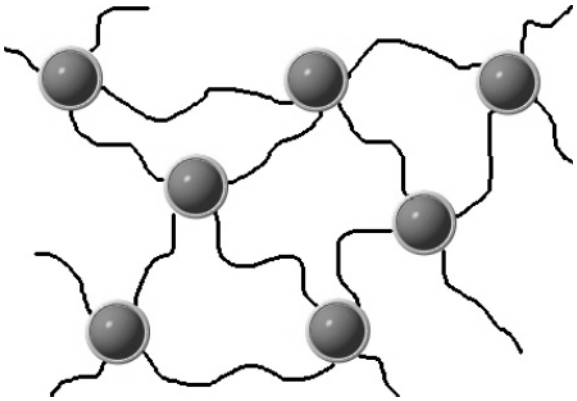

Figure 2. Phase separation structure of general commercial SEBS. The steric pellets represent the polystyrene (PS) phase and the solid lines represent the poly(ethylene-*co*-1-butene) (EB) phase, respectively. The circles around steric pellets stand for the phase interface.

* To whom all correspondence should be addressed. Telephone: +86-28-85405868. Fax: +86-28-85402465. E-mail: amzhang215@vip.sina.com.
[†] Sichuan University.
[‡] Baling Petrochemical Industry Co., Ltd., of China Sinopec.

10.1021/ma071630p CCC: $37.00
Published on Web 11/09/2007

behaviors, and the order−disorder transitions. Infrared spectroscopy (IR), of course, was employed to study SEBS, but the purpose was only to investigate the oxidation and degradation of SEBS.[23−25] In this study, we have utilized IR spectroscopy to elucidate the temperature-dependent molecular chain movements and transitions of SEBS. However, because the band intensity variation of SEBS is quite weak, we cannot obtain useful information from the temperature-dependent in situ IR spectrum. Furthermore, the IR spectra of SEBS are the overlapping of the hard block and soft block IR spectra, and therefore, the complex band intensity variation also cannot be distinguished. Even several important weak bands are usually submerged under the spectra baseline. In order to separate the overlapping bands and emphasize the important intensity variation, one should use powerful analysis methods. In the present study, we have employed moving-window two-dimensional (MW2D) correlation spectroscopy.

Thomas and Richardson introduced moving-window two-dimensional correlation spectroscopy method in 2000,[26] and therefore, the phase transition temperature of a thermotropic liquid crystal sample was determined from the temperature-dependent IR combined with the MW2D method. This method, which uses the date subdivision technique, is an extension of generalized two-dimensional correlation spectroscopy,[27−29] proposed by Noda in 1993.[30] MW2D can directly observe spectral correlation variation along both spectral variables (e.g., wavenumber) and perturbation variables (e.g., temperature) axes.[31−34] Accordingly, the transition point can be determined from the correlation intensity along the perturbation variables direction. Recently, Morita has successfully applied MW2D spectroscopy for the determination of the glass transition of PMMA,[31] as well as the melting temperature of PVA.[35] Šašić has also successfully employed MW2D spectroscopy to determine the phase-transition point of PNiPA.[34]

In this study, the temperature-dependent molecular chain movements and transitions of SEBS above room temperature were studied by infrared spectroscopy combined with moving-window two-dimensional correlation analysis. The extraordinary weak crystalline nature of $-(CH_2-CH_2)-_n$ in the EB block melting at 48 °C is discussed in detail. The heat enthalpy relaxation of S block around 72−80 °C, the glass transition of S block (atactic polystyrene) around 120 °C, and other discoveries are all elucidated at the functional group level.

2. Experimental Section

2.1. Materials. SEBS used for experiment was G1657, which was purchased from Shell Development Co. Its weight-average molecular weight is 70 000 g/mol with a polydispersity index $\bar{M}_w/M_n = 1.05$, and the soft/hard ratio is 87/13 (weight). G1657 is expected to form a body-centered cubic (bcc) sphere morphology and stated to contain roughly 30 wt % diblock copolymer. SEBS was directly used in experiment without further purification.

2.2. FTIR Spectroscopy. SEBS was spread on one side of a KBr disk via solvent casting from a 20 g/L cyclohexane solution. The KBr disk (0.8 mm thick), together with SEBS film sample, was dried in a vacuum oven at 70 °C for 60 min and the vacuum degree was −0.08 MPa. The SEBS film disk sample was placed into a homemade temperature control instrument including program heating cell and circulation water jacket cooling system. The temperature-dependent absorbance IR spectra were measured with Nicolet-560 IR spectrometer, which was equipped with a deuterated triglycine sulfate (DTGS) detector. The spectral resolution was 4 cm^{-1} and the number of scans of each spectrum was 40. The SEBS film sample was protected by dried high-purity nitrogen gas during measurement. A total of sixty-eight IR spectra were collected from 30 °C to 166 °C at approximately 2 °C increments. Simultaneously, the temperature increasing rate was 5 °C/min.

2.3. MW2D Correlation Analysis. Before performing the MW2D correlation analysis, the intensity of the each IR spectrum was normalized by dividing its intensity mean value. In the present study, all the MW2D correlation spectra were processed and calculated by two-dimensional correlation spectroscopy software, 2DCS (the latest version is 3.0, C++), developed in our laboratory. The projection of contour images of the MW2D correlation spectra in this study were also directly plotted by 2DCS 3.0. During the calculation, the window size was $2m + 1 = 11$. The 5% autocorrelation intensity of MW2D correlation spectra was regarded as noise and was cut off.

3. MW2D Correlation Spectroscopy Theory

The theory of MW2D correlation spectroscopy has been described elsewhere.[31] Here, we express it as follows.

The MW2D method is essentially the division of a spectral intensity data matrix into a series of submatrices. Each of submatrices is regarded as a window. We consider $W(\upsilon,I)$ as an $M \times N$ spectral intensity data matrix, where υ and I are the spectral variable (e.g., wavenumber) and the perturbation variable (e.g., temperature), respectively. Each row of $W(\upsilon,I)$ corresponds to one spectrum. The number of rows and columns of the spectral intensity data matrix are M and N, respectively. What calls for special attention is that the spectral intensity in $W(\upsilon,I)$ is normalized by dividing the mean value of each row that it locates.

$$W(\upsilon,I) = \begin{pmatrix} y(\upsilon_1,I_1) & y(\upsilon_2,I_1) & \cdots & y(\upsilon_{N-1},I_1) & y(\upsilon_N,I_1) \\ \vdots & \vdots & \cdots & \vdots & \vdots \\ y(\upsilon_1,I_j) & y(\upsilon_2,I_j) & \cdots & y(\upsilon_{N-1},I_j) & y(\upsilon_N,I_j) \\ \vdots & \vdots & \cdots & \vdots & \vdots \\ y(\upsilon_1,I_M) & y(\upsilon_2,I_M) & \cdots & y(\upsilon_{N-1},I_M) & y(\upsilon_N,I_M) \end{pmatrix} \quad (1)$$

Now, a submatrix $w_j(\upsilon,I)$ is extracted around the jth row of the main matrix (eq 1). The index range of the perturbation variable I is from j-m to j+m, apparently, w_j (υ,I) has $2m + 1$ (window size) rows and its column is equal to that of $W(\upsilon,I)$.

$$w_j(\upsilon,I) = \begin{pmatrix} y(\upsilon_1,I_{j-m}) & y(\upsilon_2,I_{j-m}) & \cdots & y(\upsilon_{N-1},I_{j-m}) & y(\upsilon_N,I_{j-m}) \\ \vdots & \vdots & \cdots & \vdots & \vdots \\ y(\upsilon_1,I_j) & y(\upsilon_2,I_j) & \cdots & y(\upsilon_{N-1},I_j) & y(\upsilon_N,I_j) \\ \vdots & \vdots & \cdots & \vdots & \vdots \\ y(\upsilon_1,I_{j+m}) & y(\upsilon_2,I_{j+m}) & \cdots & y(\upsilon_{N-1},I_{j+m}) & y(\upsilon_N,I_{j+m}) \end{pmatrix} \quad (2)$$

In general, the reference spectrum and dynamic spectrum in the jth submatrix (window) are calculated according to eqs 3 and 4.

$$\bar{y}(\upsilon) = \frac{1}{2m+1}\sum_{J=j-m}^{j+m} y(\upsilon,I_J) \quad (3)$$

$$\tilde{y}(\upsilon,I_J) = y(\upsilon,I_J) - \bar{y}(\upsilon) \quad (4)$$

Here, J corresponds to the index of rows within a submatrix. The mean-centered jth submatrix is obtained.

$$\tilde{w}_j(\upsilon,I) = \begin{pmatrix} \tilde{y}(\upsilon_1,I_{j-m}) & \tilde{y}(\upsilon_2,I_{j-m}) & \cdots & \tilde{y}(\upsilon_{N-1},I_{j-m}) & \tilde{y}(\upsilon_N,I_{j-m}) \\ \vdots & \vdots & \cdots & \vdots & \vdots \\ \tilde{y}(\upsilon_1,I_j) & \tilde{y}(\upsilon_2,I_j) & \cdots & \tilde{y}(\upsilon_{N-1},I_j) & \tilde{y}(\upsilon_N,I_j) \\ \vdots & \vdots & \cdots & \vdots & \vdots \\ \tilde{y}(\upsilon_1,I_{j+m}) & \tilde{y}(\upsilon_2,I_{j+m}) & \cdots & \tilde{y}(\upsilon_{N-1},I_{j+m}) & \tilde{y}(\upsilon_N,I_{j+m}) \end{pmatrix} \quad (5)$$

Table 1. Wavenumbers of Interest Bands of SEBS IR Spectrum and Bands Assignment Divided into EB and S Blocks

	assignment	
wavenumber (cm^{-1})	EB block	S block
2960[38−40]	C−H asymmetry stretching, $-CH_3$	
2923[37]	C−H asymmetry stretching, $-CH_2-$	C−H asymmetry stretching of fundamental chain, $-CH_2-$
2852[37]	C−H symmetry stretching, $-CH_2-$	C−H symmetry stretching of fundamental chain, $-CH_2-$
1600[37]		$V_{9B}(B_1)$ framework vibration of the side benzene ring
1594[47]		overtone or combination vibration of the side benzene ring
1585[37]		$V_{9A}(A_1)$ framework vibration of the side benzene ring
1575[47]		overtone or combination vibration of the side benzene ring
1568[47]		overtone or combination vibration of the side benzene ring
1461[37−40]	C−H bending, $-CH_2-$	
1378[38−40]	C−H bending, $-CH_3$	
1263[43−46]		vibration of the helical structure in crystals
1195[37]		$\upsilon_{8A}(A_1)$ vibration of the side benzene ring
1157[37]		$\upsilon'_{15}(B_1)$ vibration of the side benzene ring
762[37]		═C−H bending vibration of side benzene ring
721[37, 41, 42]	C−H rocking, $-CH_2-$	
700[37]		═C−H bending vibration of side benzene ring

Then, synchronous and asynchronous generalized two-dimensional correlation spectra are calculated from $\tilde{w}_j(\upsilon,I)$ according to eq 6 and eq 7.

$$\Phi_j = \frac{1}{2m}[\tilde{w}_j(\upsilon,I)]^T \cdot [\tilde{w}_j(\upsilon,I)] \tag{6}$$

$$\Psi_j = \frac{1}{2m}[\tilde{w}_j(\upsilon,I)]^T \cdot H \cdot [\tilde{w}_j(\upsilon,I)] \tag{7}$$

where $[\tilde{w}_j(\upsilon,I)]^T$ is the transposed matrix of $\tilde{w}_j(\upsilon,I)$ and H is the Hilbert−Noda[36] transformation matrix ($(2m + 1) \times (2m + 1)$) defined as follows:

$$h_{ik} = \begin{cases} 0 & i = k \\ \dfrac{1}{\pi(k-i)} & \text{otherwise} \end{cases} \tag{8}$$

where h_{ik} is the element of the ith row and the kth column of matrix H.

The MW2D correlation spectrum is obtained through sliding window position from $j = 1 + m$ to $M - m$ and repeating calculations of eqs 2−7 at each window.

For the MW2D correlation spectrum based on an autocorrelation spectrum, each row ($\Omega_{A,j}(\upsilon,I_j)$) of MW2D correlation spectrum matrix is directly extracted from a diagonal line of Φ_j matrix, namely, the autocorrelation intensity of synchronous 2D correlation spectrum at the same two spectral variables $\Phi_j(\upsilon,\upsilon)$. Undergoing the procedure mentioned above from $j = 1 + m$ to $M - m$, the MW2D correlation spectrum matrix $\Omega_A(\upsilon,I)$, based on an autocorrelation spectrum, can be obtained conveniently. The MW2D correlation spectrum based on an autocorrelation spectrum describes the variance of a spectral intensity change induced by an external perturbation (e.g., temperature).

For the MW2D correlation spectrum based on a slice spectrum, each row ($\Omega_{\Phi,j}(\upsilon,I_j)$) of synchronous MW2D correlation spectrum matrix, as well as each row ($\Omega_{\Psi,j}(\upsilon,I_j)$) of asynchronous MW2D correlation spectrum matrix, is extracted from a fixed row of Φ_j and Ψ_j matrixes, respectively, for example, $\upsilon_2 = \upsilon_f$. In this case, $\Phi_j(\upsilon,\upsilon_f)$ and $\Psi_j(\upsilon,\upsilon_f)$ are used. Likewise, for the sliding window position from $j = 1 + m$ to $M - m$, $\Omega_\Phi(\upsilon,I)$ and $\Omega_\Psi(\upsilon,I)$ matrixes are obtained easily. The MW2D correlation spectrum based on a slice spectrum can distinguish synchronous and asynchronous correlations between spectral variables and perturbation variables; however, the selection of the fixed υ_f is very important in regards to the system under investigation.

4. Results and Discussion

There are several bands of the IR spectrum of SEBS that are of interest to our study. The IR spectrum of SEBS is the overlapping of S block (atactic polystyrene) and EB block (poly(ethylene-*co*-1-butene)) IR spectra (not displayed here). According to the literature,[37−47] the bands assignment of SEBS spectrum are summarized in Table 1.

4.1. Weak Crystalline Melting of EB Block. The normalized temperature-dependent IR spectra in the 780−670 cm^{-1} region of SEBS are shown in Figure 3 (30−166 °C). For clarity, the whole spectra are not shown. The thick spectrum curve is the first collected spectrum (at 30 °C). The peaks at 700 and 762 cm^{-1} are assigned to the ═C−H bending vibration of the side benzene ring of S block. It can be observed from Figure 3 that the peak at 762 cm^{-1} shifts to lower wavenumbers and the intensity at peak 700 cm^{-1} decreases as the temperature increases; The peak at 721 cm^{-1} assigned to $-CH_2-$ rocking vibration of EB block decreases explicitly from an obvious peak to a straight line.

Figure 4 shows the MW2D correlation spectrum based on autocorrelation calculations in the 780−670 cm^{-1} region. At 48 °C, three positive correlation intensity peaks are observed. As mentioned above, 721 cm^{-1} is assigned to the C−H rocking vibration of the $-CH_2-$ of EB block. It indicates that the extraordinary weak crystalline of EB block of SEBS melts at 48 °C. Generally, the weak crystalline of $-(CH_2-CH_2)-_n$ of EB block should exist in continuous phase (soft block EB), and therefore it has no relation with disperse phase (hard block S). However, at 48 °C, the correlation intensity peaks at 700 cm^{-1}

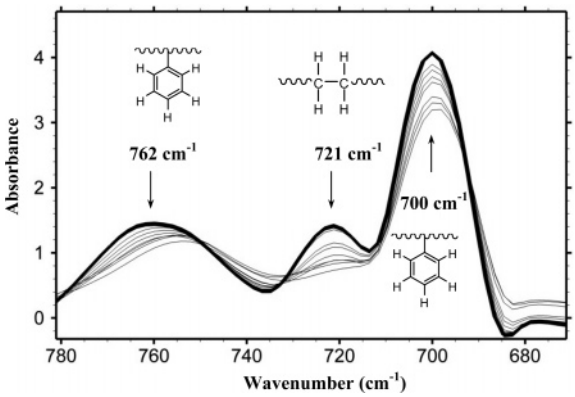

Figure 3. Normalized temperature-dependent IR spectra in the 780−670 cm^{-1} region of SEBS (30−166 °C). The thick spectrum curve is the first collected spectrum (at 30 °C).

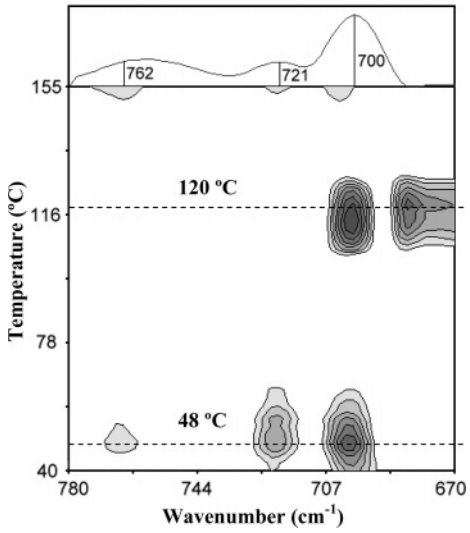

Figure 4. MW2D correlation spectrum based on autocorrelation calculated from the temperature-dependent IR spectra of SEBS (30−166 °C) in the region 780−670 cm^{-1}. The curve in the top rectangle is a corresponding static IR spectrum of SEBS. The contour levels represent the projection of MW2D correlation intensity. The horizontal dashed lines correspond to the temperature point at 48 and 120 °C, respectively.

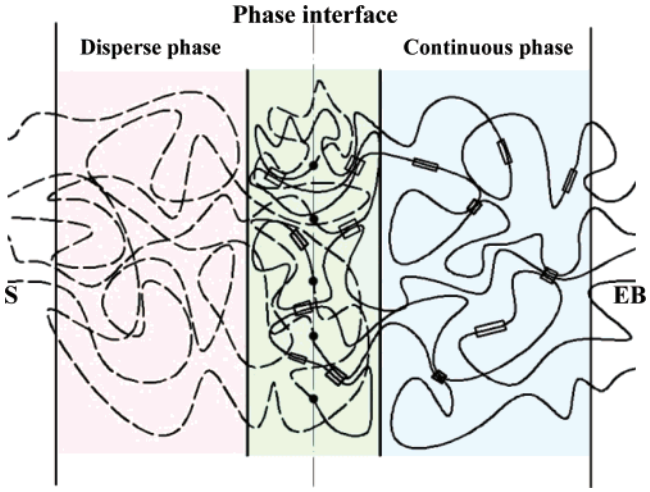

Figure 5. Sketch map of SEBS and the ambient temperature is below 40 °C. The dashed lines represent polystyrene (PS) and the solid lines represent poly(ethylene-*co*-1-butene) (EB), respectively. The solid round dots stand for chemical joint between polystyrene and poly(ethylene-*co*-1-butene). The small rectangle boxes, through which are drilled by EB molecular chains, stand for the very weak crystalline in EB. The center area between two vertical heavy lines is the phase interface.

and 762 cm^{-1} assigned to the ═C−H bending vibration of the side benzene ring of S block appear simultaneously. It can be speculated that a few of the polystyrene chain segments surround some weak crystalline domain of EB block. The unique location, which meets the condition mentioned above, is the interface between the S and EB blocks. This phase interface is a transitional region, and therefore the chain segment of S and EB block coexist. During the extraordinary weak crystalline of EB block melting within phase interface, the chain segment of S block around weak crystalline is influenced. Of course, this type of weak crystalline comes into existence within phase interface and continuous phase simultaneously. Figure 5 illustrates the state of the interface and the ambient temperature is below 40 °C. It can be easily explained why at 700, 721, and 762 cm^{-1} the positive correlation intensity peaks appear at the same time. Recently, some researchers have studied the melting

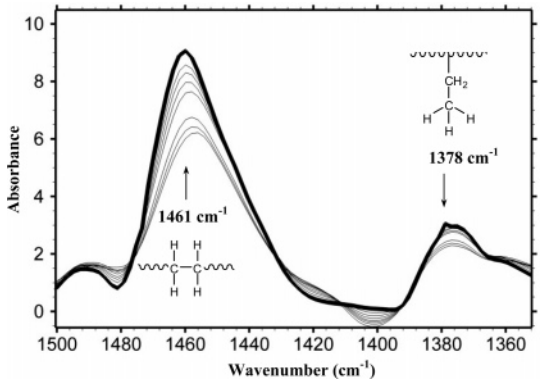

Figure 6. Normalized temperature-dependent IR spectra in the 1500−1350 cm^{-1} region of SEBS (30−166 °C). The thick spectrum curve is the first collected spectrum (at 30 °C).

temperature of EB weak crystals.[42,48−51] These studies showed that because of incompleteness of the weak crystals, the melting temperature of the weak crystals deceases with the content of the ethyl branches increasing. When the number of ethyl branches per 1000 backbone C atoms is within 45−75, with respect to the difference of samples and experimental conditions, the measurement value of these studies ranges from 25 to 55 °C. The EB block of G1657 has 71 ethyl branches per 1000 backbone C atoms; apparently, 48 °C obtained from the MW2D correlation spectrum is within the range mentioned above. The melting temperature of EB weak crystals reported by Jokela (DSC measurement)[48] is 47 °C, and this value is close to our result.

4.2. The Glass Transition of the S Block. As shown in Figure 4, around 120 °C, two positive correlation intensity peaks are observed at 700 and 687 cm^{-1} which are assigned to the ═C−H bending vibration of the side benzene ring of S block. It is obviously a consequence of the S block glass transition. It is known that the classical glass transition temperature of atactic polystyrene is about 100 °C.[52,53] As a matter of fact, the S block of SEBS is also the atactic polystyrene (but monodispersity). Why is the glass transition temperature of S block measured by MW2D around 120 °C and not at 100 °C? This can be explained as follows. The glass state of random polymers is thermodynamic nonequilibrium and time-dependent, and therefore, it is easily influenced by measuring conditions (heating speed, scanning frequency). Near the glass transition, the value change of some physical quantities (heat absorption capacity, modulus of elasticity, thermal coefficient of expansion, and so on) of random polymers occurs accidentally, and therefore the different test methods (DSC, DMTA and so on) collect the value change of the different physical quantities. Moreover, the temperature response speed of each physical quantity also has distinctness. Therefore, the measurement values of glass transition temperature always have differences due to the different test methods and measuring conditions. In this study, first, the dipole movement variation of SEBS chains (with the temperature increasing) is revealed by MW2D. Second, the response speed of the dipole movement is also different at the different heating speed. It is estimated that changing the measuring conditions, for example, decreasing the heating speed, will yield a similar value (to compare with DSC or DMTA).

The normalized temperature-dependent IR spectra in the 1500−1350 cm^{-1} region are shown in Figure 6 (30−166 °C). For clarity, the whole spectra are not shown. The thick spectrum curve is the first collected spectrum (at 30 °C).

The peaks at 1461 $cm^{-1}$and 1378 cm^{-1} require special attention. The former is assigned to the C−H bending vibration

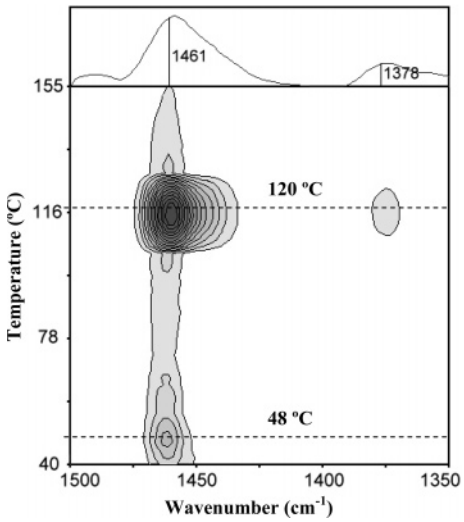

Figure 7. MW2D correlation spectrum based on autocorrelation calculated from the temperature-dependent IR spectra of SEBS (30−166 °C) in the region 1500−1350 cm^{-1}. The curve in the top rectangle is a corresponding static IR spectrum of SEBS. The contour levels represent the projection of MW2D correlation intensity. The horizontal dashed lines correspond to the temperature point at 48 and 120 °C, respectively.

of $-CH_2-$ of the EB block and the latter is assigned to the C−H bending vibration of $-CH_3$ of the ethyl branches of the EB block. Figure 7 shows the MW2D correlation spectrum based on autocorrelation calculations in the 1500−1350 cm^{-1} region. It can be observed that a positive intensity peak at 1461 cm^{-1} appears at 48 °C, and this intensity corresponds to the intensity at 721 cm^{-1} in Figure 4. Both of them indicate the melting of extraordinary weak crystals of $-(CH_2-CH_2)-_n$ of the EB block. However, we found that, around 120 °C, the bands at 687 and 700 cm^{-1} assigned to the S block, as well as the bands at 1461 and 1378 cm^{-1} assigned to the EB block, show the maximum positive correlation intensity peaks (Figures 4 and 7). As discussed above, SEBS (G1657) is a type of phase separation block copolymer and a phase interface exist in the transitional region between EB and S block. It can be speculated that, within this interface, the movement of the chain segment of S block will drive the chain segment of EB block to move.

In order to reveal the mechanism of the phenomenon mentioned above, the MW2D correlation spectrum, based on a slice spectrum in the 1500−1350 cm^{-1} region, was calculated. The slice point: $\upsilon_f = 700$ cm^{-1}, assigned to the =C−H bending vibration of the side benzene ring of S block, and other parameters are all the same as section 2.3. Parts a and b of Figure 8 show the synchronous MW2D correlation spectrum and the asynchronous MW2D correlation spectrum. The filled and unfilled areas correspond to the positive and the negative correlation intensity, respectively. Figure 8a is similar to Figure 7, and Figure 8b is nosier than Figure 8a. Around 120 °C, as shown in Figure 8, parts a and b, Ω_Φ (1461 cm^{-1}, 120 °C) > 0, Ω_Ψ(1461 cm^{-1}, 120 °C) < 0 and Ω_Φ (1378 cm^{-1}, 120 °C) > 0, Ω_Ψ(1378 cm^{-1}, 120 °C) < 0. According to the rules given by Noda,[30] the intensity changes at bands 1461 and 1378 cm^{-1} occur after the changes at 700 cm^{-1}. This indicates that the chain segment movement of S block does indeed occur before that of EB block during S block glass transition. The probable mechanism can be expressed as follows. (1) At the onset of the S block glass transition, some chain segment of S block initiate movement. (2) When the temperature increases, this kind of increased movement gradually spreads to the phase interface between S and EB block. (3) Due to the connection of the

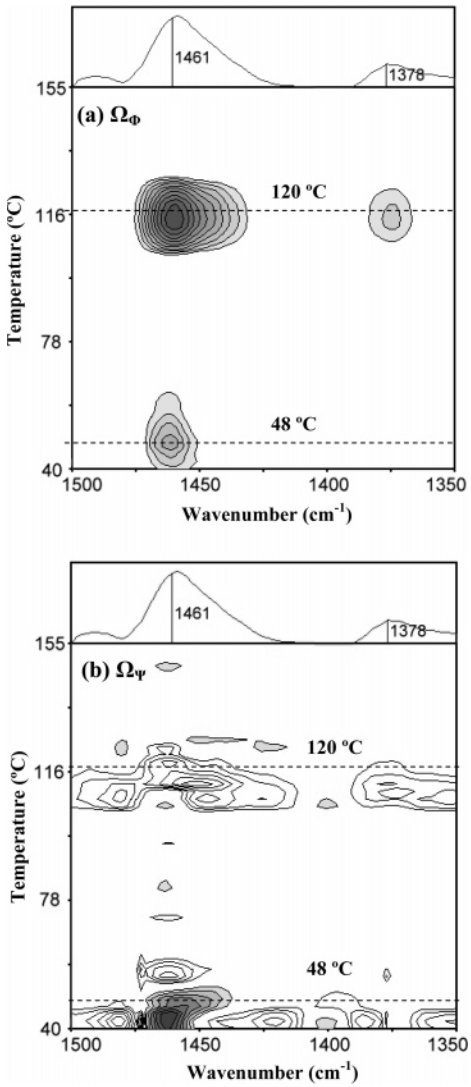

Figure 8. MW2D correlation spectra based on a slice spectrum calculated from the temperature-dependent IR spectra of SEBS (30−166 °C) in the region 1500−1350 cm^{-1}. The contour levels represent the projection of MW2D correlation intensity. The horizontal dashed lines correspond to the temperature point at 48 and 120 °C. The filled and unfilled areas correspond to the positive and the negative correlation intensity, respectively. The slice point, $\upsilon_f = 700$ cm^{-1}, which is assigned to the =C−H bending vibration of the side benzene ring of S block. Key: (a) synchronous MW2D correlation spectrum; (b) asynchronous MW2D correlation spectrum.

chemical structure, the chain segment movement of S block drives the chain segment of EB block to move within the interface. At the same time, the area of the interface broadens and the chemical joints initiate the deviation from the equilibrium position. Furthermore, the resistance force of chain segment interdiffusion between S and EB block reaches a maximum. (4) When the temperature keeps on increasing, the resistance force of chain segment diffusion (within the interface) gradually decreases, and the area of the interface broadens further (until it is stabilized). Meanwhile, the chain segment of EB block, which is close to the interface, is driven to move and enters into the interface. Figure 9 illustrates the state of the phase interface during the glass transition of the S block.

4.3. The Polystyrene Fundamental Chains of the Disperse Phase (S Block) Center Initiating a Complete Move. The normalized temperature-dependent IR spectra in the 3000−2800 cm^{-1} region are shown in Figure 10 (30−166 °C). The peak at 2960 cm^{-1} is assigned to the C−H asymmetry stretching

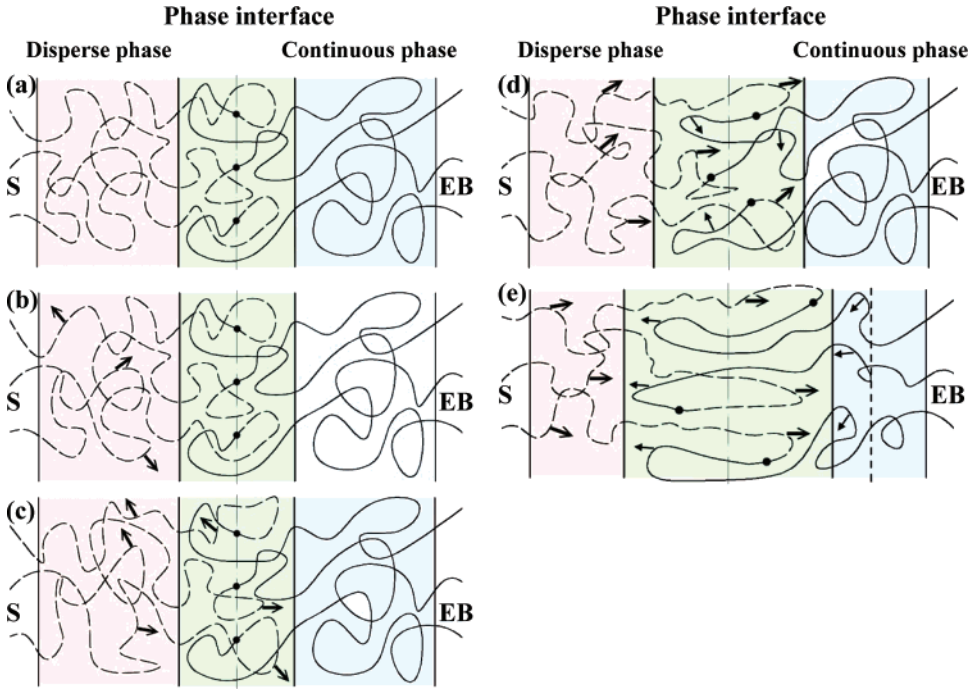

Figure 9. Sketch map of SEBS during the glass transition of S block. The dashed lines represent polystyrene (PS) and the solid lines represent poly(ethylene-*co*-1-butene) (EB). The solid round dots stand for chemical joint between polystyrene and poly(ethylene-*co*-1-butene). The big and small arrows show the movement direction of chain segment of S block and that of EB block, respectively. Key: (a) temperature below glass transition; (b) onset of glass transition; (c) increased movement of S block spreading to the interface; (d) chain segment movement of S block driveing the chain segment of EB block to move within the interface with the area of the interface broadening; (e) interface broadening further, meanwhile, the chain segment of EB block which is close to the interface is driven to move and enters into the interface.

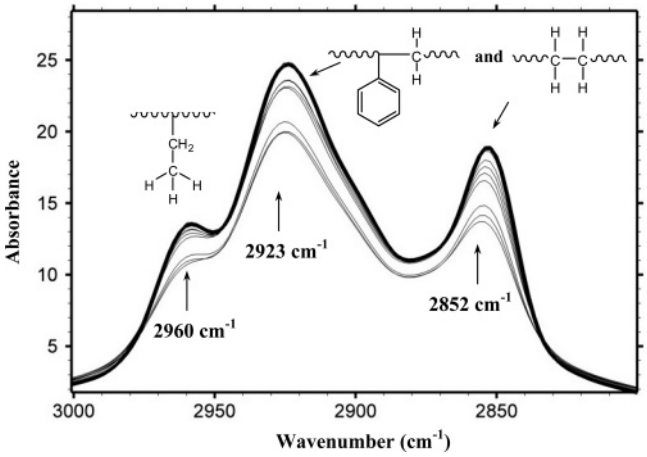

Figure 10. Normalized temperature-dependent IR spectra in the 3000−2800 cm^{-1} region of SEBS (30−166 °C). The thick spectrum curve is the first collected spectrum (at 30 °C).

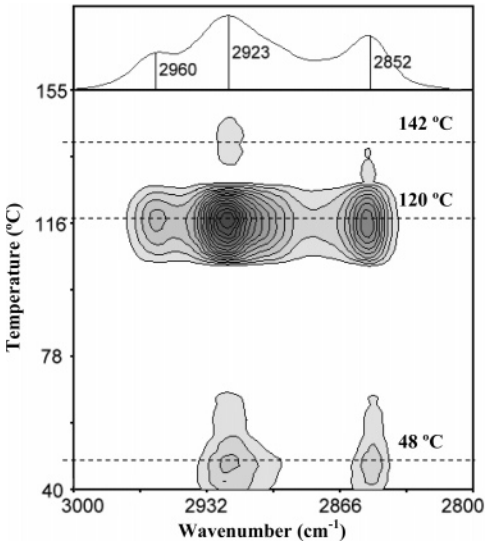

Figure 11. MW2D correlation spectrum based on autocorrelation calculated from the temperature-dependent IR spectra of SEBS (30−166 °C) in the region 3000−2800 cm^{-1}. The curve in the top rectangle is a corresponding static IR spectrum of SEBS. The contour levels represent the projection of MW2D correlation intensity. The horizontal dashed lines correspond to the temperature points at 48, 120, and 142 °C.

vibration of $-CH_3$ of ethyl branches of EB block. The peaks at 2923 cm^{-1} and 2852 cm^{-1} are assigned to the C−H asymmetry and symmetry stretching vibration of $-CH_2-$, both in EB and S block fundamental chains.

Figure 11 shows the MW2D correlation spectrum based on autocorrelation calculations in the 3000−2800 cm^{-1} region. It can be observed that, at 2923 and 2852 cm^{-1}, two weak positive correlation intensity peaks appear at 48 °C and they correspond to the melting of extraordinary weak crystals of $-(CH_2-CH_2)-_n$ of the EB block. The other results are the same as discussed in sections 4.1 and 4.2. However, around 142 °C a weak positive correlation intensity peak is observed at 2923 cm^{-1}. Krishnamoorti group[54−56] reported the "worm like" cylinder-to-sphere order−order transition (OOT) of SEBS was within 135−141 °C. However, in their study the annealing time spent by OOT reached 24−72 h. In our experiment, the SEBS film sample on the KBr disk was cast from the cyclohexane solution and it was dried for only 60 min at 70 °C. The heating time (30−166 °C) was also only 27.2 min. Thus, in our experimental condition, the OOT reported by Krishnamoorti group seems impossible. The correlation intensity peak at 142 °C has its origins from the movement of $-CH_2-$ of fundamental chains; we prefer to assign it to the movement of $-CH_2-$ of S block fundamental chains at this high temperature.

From this viewpoint, the transition mechanism of SEBS at 142 °C may be similar to the one mentioned above: the

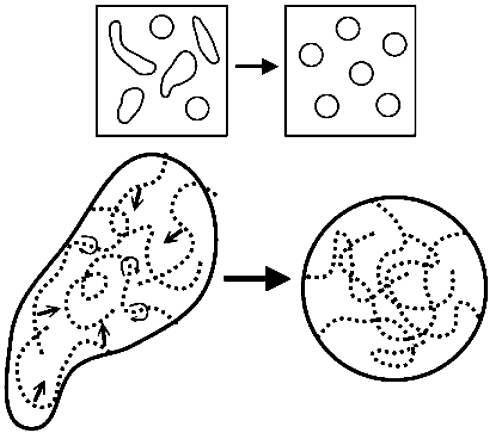

Figure 12. At 142 °C, a fraction of disperse phase (S block) of SEBS deform from incomplete shape to sphere through the polystyrene fundamental chain movements and the conformation modifications. The dashed lines represent the polystyrene fundamental chains. The straight arrows and the arc-shaped arrows represent the motion direction and the conformation modifications direction of polystyrene fundamental chains, respectively.

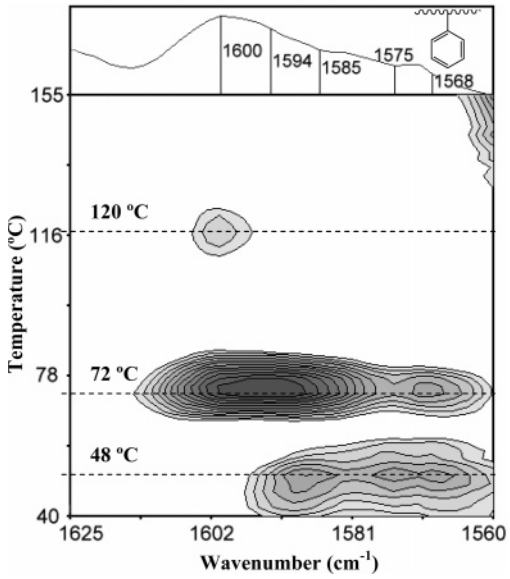

Figure 13. MW2D correlation spectrum based on autocorrelation calculated from the temperature-dependent IR spectra of SEBS (30−166 °C) in the region 1625−1560 cm^{-1}. The curve in the top rectangle is a corresponding static IR spectrum of SEBS. The contour levels represent the projection of MW2D correlation intensity. The horizontal dashed lines correspond to the temperature point at 48, 72, and 120 °C. All the bands are assigned to the side benzene ring of the S block.

polystyrene fundamental chains, in a fraction of disperse phase (S block) center, begin to move entirely, and therefore through the polystyrene fundamental chain movements and the free conformation modifications, a fraction of the disperse phase deforms from an incomplete shape to a sphere (Figure 12). The temperature, at 142 °C, can be explained as the polystyrene fundamental chains of disperse phase (S block) center initiating to completely move. This corresponds to the entirely viscous flow temperature of the fundamental chains of the S block.

4.4. The Heat Enthalpy Relaxation of S Block. Figure 13 shows the MW2D correlation spectrum based on autocorrelation calculations in the 1625−1560 cm^{-1} region. The peaks at 1600, 1594, and 1568 cm^{-1} are of interest to us. The 1600, 1594, and 1568 cm^{-1} peaks are assigned to the framework vibration of the side benzene ring of S block. Around 72 °C, positive correlation intensity at 1600, 1594, and 1568 cm^{-1} was observed

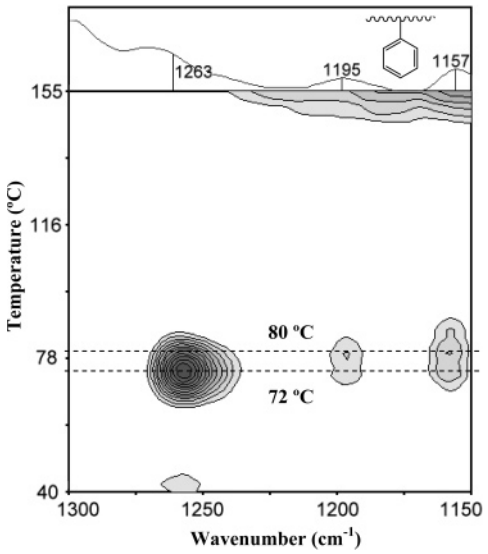

Figure 14. MW2D correlation spectrum based on autocorrelation calculated from the temperature-dependent IR spectra of SEBS (30−166 °C) in the region 1300−1150 cm^{-1}. The curve in the top rectangle is a corresponding static IR spectrum of SEBS. The contour levels represent the projection of MW2D correlation intensity. The horizontal dashed lines correspond to the temperature point at 72 and 80 °C, respectively. All the bands are assigned to the side benzene ring of S block.

(Figure 13). This indicates that the local structure of S block proceeds relaxation movement around 72 °C. This phenomenon is also called the relaxation below the glass transition.[57−59] In this study, we found that the movement of the side benzene ring of S block brings this type of heat enthalpy relaxation. Moreover, the movement is only confined to the framework vibration of the side benzene ring. Hence, around 72 °C, the positive intensity is never observed at all in Figures 4, 7, and 11.

Here, the assignment of 1594 and 1568 cm^{-1} should be discussed in detail. Recently, Paul Painter[47] has employed IR and the peak-fit method to investigate vibration relaxation of atactic polystyrene. They reported two new bands at 1594 and 1575 cm^{-1} which are assigned to the overtone or combination vibration of the side benzene ring. In their research, the peak at 1575 cm^{-1} was extraordinary weak, but in order to gain a good curve fit, this band cannot be omitted, In this study, we also found these two bands at 1594 and 1575 cm^{-1} in Figure 13. Besides, a new band at 1568 cm^{-1} was observed. As the temperature increases from 48 to 72 °C, the peaks at 1575 and 1565 cm^{-1} merge into one peak at 1568 cm^{-1}. There is no doubt that the peak at 1568 cm^{-1} should be assigned to the overtone or combination vibration of the side benzene ring of S block. As discussed above, the MW2D correlation spectrum has high resolution to determine new bands.

Figure 14 shows the MW2D correlation spectrum based on autocorrelation calculations in the 1300−1150 cm^{-1} region. The peaks at 1195 and 1157 cm^{-1} are assigned to the framework vibration of the side benzene ring of S block. At 80 °C, two positive correlation intensity peaks at 1195 and 1157 cm^{-1} are observed and this also indicates the local structure relaxation movement of S block. What calls for special attention is that, at 72 °C, a maximum positive correlation intensity peak at 1263 cm^{-1} is observed in Figure 14. The peak at 1263 cm^{-1} was found to appear in the crystalline state and also the gel state of isotactic polystyrene; however, it did not appear in the amorphous state of isotactic polystyrene.[44−46] Thus, some researchers consider the peak at 1263 cm^{-1} to be the helical structure of

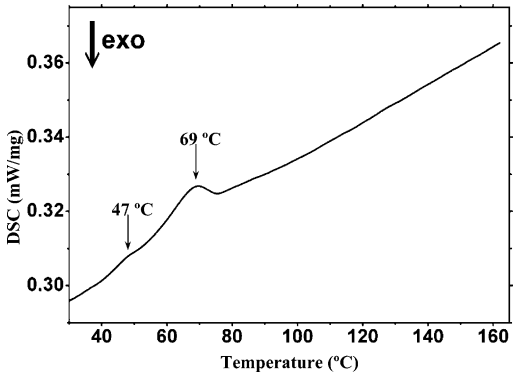

Figure 15. DSC curve of SEBS (G1657) from 30 to 170 °C and the heating rate is 10 °C/min.

isotactic polystyrene crystalline.[44,45] This indicates directly that the very weak crystalline (at least local ordered) exists in the amorphous S block of SEBS and this kind of weak crystalline melts at 72 °C. Some researchers[43] found the peak at 1263 cm^{-1} appeared in the IR spectrum of the monodisperse freeze-dried atactic polystyrene. In fact, S block of SEBS is also monodisperse. We conclude that not only heat enthalpy relaxation of S block, but also the melting of the weak crystalline of S block is at 72 °C.

4.5. To Compare with DSC Measurement of SEBS (G1657). Finally, the DSC curve of SEBS (G1657) is shown in Figure 15. NETCZH DSC-204 was used. The heating rate was 10 °C/min and the experimental temperature range was 30−170 °C. SEBS sample was protected by dried high-purity nitrogen gas during measurement. From 30 to 170 °C, there are two endothermic peaks observed, 47 and 69 °C, respectively. The peak at 47 °C is weak. The former corresponds to the melting of $-(CH_2-CH_2)-_n$ of EB block, the latter corresponds to the heat enthalpy relaxation of S block, which is induced by the framework movement of the side benzene ring and the melting of the very weak crystalline of S block. These two results are the same as revealed by MW2D correlation spectra. When the experimental temperature is above 80 °C, the DSC curve of SEBS becomes a sloping straight line, and therefore the glass transition temperature of S block cannot be determined as well as other information. Because the ratio of soft/hard in G1657 is 87/13 (weight), the indetermination of glass transition temperature of S block is reasonable.[19,22] We repeated the DSC measurement three times, and the results were uniform.

5. Conclusion

In the present study, MW2D correlation spectroscopy was employed to study the temperature-dependent IR of SEBS above room temperature. Some complex molecular chain movements and transitions of SEBS were revealed with a linear increment temperature increasing (30−166 °C).

(1) At 48 °C, the extraordinary weak crystal of $-(CH_2-CH_2)-_n$ of the EB block melts. At the same time, the melting of this crystalline within phase interface drives the side benzene ring of S block, in the phase interface, to move.

(2) At 72−80 °C, the heat enthalpy relaxation of S block, which is induced by the framework movement of the side benzene ring and the melting of the very weak crystal of the S block, is observed from the MW2D correlation spectrum.

(3) At 120 °C, the glass transition of the S block, the chain segment movement of the S block occurs before that of EB block in phase interface.

(4) 142 °C, the fundamental chains of disperse phase (S block) center initiate complete movement, and this type of movement drives a fraction of the disperse phase to deform from an incomplete shape to a sphere. This corresponds to the entirely viscous flow temperature of the fundamental chains of the S block.

From the discussion of the present study, it can be concluded that the information, which is revealed by the temperature-dependent IR combined with MW2D correlation analysis, is far more fine and complex than that from DSC or other measurements. Although the investigated subject of MW2D correlation spectroscopy is microscopic and submicroscopic molecular dipole movements, the observed results can be easily be concluded to be due the variation of meso or macroscopic physical characteristics of materials. MW2D correlation spectroscopy is the expansion and extension of the generalized two-dimensional correlation method. If the research target of the generalized two-dimensional correlation method is the microscopic and submicroscopic molecular movement law, then MW2D correlation spectroscopy has become the connection between the microscopic law and the variation law of the macroscopic physical characteristics. As far as this statement is concerned, MW2D correlation spectroscopy is significant. Recently, Ozaki and Noda have introduced perturbation-correlation moving-window two-dimensional correlation spectroscopy (PCMW2D),[35,60,61] which is a further extension of MW2D.

Because of the limitation of the temperature control system in the IR sample cell, the temperature range of the IR experiment is only from 30 to 166 °C in this paper, namely, above room temperature. As a matter of fact, the glass transition temperature of the EB block is from −50 to −60 °C; furthermore, there are several secondary transitions about the S block below 0 °C. We believe, if the experimental temperature range is from −100 to 0 °C, that the molecular chain movements and transitions of SEBS will be finely elucidated with MW2D correlation spectroscopy. The method, which is employed in our present study, can be conveniently transferred to other block copolymers, random copolymers, and homopolymers, and it will be the next research target of our research group.

Acknowledgment. This work was supported by the SEBS Microstructure Optimization Project (J404003, 05H238) of Baling Petrochemical Industry Co., Ltd., of China Sinopec. This work was also supported by the Chinese National Programs for High Technology Research and Development (2003AA333020).

References and Notes

(1) Holden, G.; Legge, N. R.; Quirk, R.; Schroeder, H. E. *Thermoplastic Elastomers*, 2nd ed.; Hanser: Munich, Germany, 1996.
(2) Walker, B. M.; Rader, C. P. *Handbook of Thermoplastic Elastomers*, 2nd ed.; Van Nostrand Reinhold: New York, 1988.
(3) Noshay, A.; McGrath, J. E. *Block Copolymers, Overview and Critical Survey*; Academic Press: New York, 1977.
(4) Morton, M. *Anionic Polymerization: Principles and Practice*; Academic Press: New York, 1983.
(5) McGrath, J. E. *Anionic Polymerization, Kinetics, Mechanisms, and Synthesis*; ACS Symposium Series 166; American Chemical Society: Washington, DC, 1981.
(6) Matsen, M. W.; Bates, F. S. *Macromolecules* **1996**, *29*, 1091−1098.
(7) Bates, F. S.; Fredrickson, G. H. *Phys. Today* **1999**, *52*, 32−38.
(8) Khandpur, A. K.; Forster, S.; Bates, F. S.; Hamley, I. W.; Ryan, A. J.; Bras, W.; Almdal, K.; Mortensen, K. *Macromolecules* **1995**, *28*, 8796−8806.
(9) Breiner, U.; Krappe, U.; Stadler, R. *Macromol. Rapid Commun.* **1996**, *17*, 567−575.
(10) Motomatsu, M.; Mizutani, W.; Tokumoto, H. *Polymer* **1997**, *38*, 1779−1785.
(11) Matsen, M. W. *J. Chem. Phys.* **1998**, *108*, 785−796.
(12) Mortensen, K.; Theunissen, E.; Kleppinger, R.; Almdal, K.; Reynaers, H. *Macromolecules* **2002**, *35*, 7773−7781.

(13) Jeong, U.; Lee, H. H.; Yang, L. H.; Kim, J. K.; Okamoto, S.; Aida, S.; Sakurai, S. *Macromolecules* **2003**, *36*, 1685−1693.
(14) Xu, Z. W.; Liang, Y. C.; Dong, S.; Cao, Y. Z.; Zhao, T. Q.; Wang, J. H.; Zhao, Q. L. *Ultramicroscopy* **2005**, *105*, 72−78.
(15) Han, X.; Hu, J.; Liu, H. L.; Hu, Y. *Langmuir* **2006**, *22*, 3428−3433.
(16) Wang, L.; Hong, S.; Hu, H. Q.; Zhao, J.; Han, C. C. *Langmuir* **2007**, *23*, 2304−2307.
(17) Wang, Y.; Shen, J. S.; Long, C. F. *Polymer* **2001**, *42*, 8443−8446.
(18) Mortensen, K.; Almdal, K.; Kleppinger, R.; Mischenko, N.; Reynaers, H. *Physica B* **1998**, *241*, 1025−1028.
(19) Sierra, C. A.; Galan, C.; Fatou, J. G.; Parellada, M. D.; Barrio, J. A. *Polymer* **1997**, *38*, 4325−4335.
(20) Baetzold, J. P.; Koberstein, J. T. *Macromolecules* **2001**, *34*, 8986−8994.
(21) Heck, B.; Arends, P.; Ganter, M.; Kressler, J.; Stuhn, B. *Macromolecules* **1997**, *30*, 4559−4566.
(22) Kim, J. K.; Lee, H. H.; Sakurai, S.; Aida, S.; Masamoto, J.; Nomura, S.; Kitagawa, Y.; Suda, Y. *Macromolecules* **1999**, *32*, 6707−6717.
(23) Allen, N. S.; Edge, M.; Wilkinson, A.; Liauw, C. M.; Mourelatou, D.; Barrio, J.; Martinez-Zaporta, M. A. *Polym. Degrad. Stab.* **2000**, *71*, 113−122.
(24) Allen, N. S.; Edge, M.; Mourelatou, D.; Wilkinson, A.; Liauw, C. M.; Parellada, M. D.; Barrio, J. A.; Quiteria, V. R. S. *Polym. Degrad. Stab.* **2003**, *79*, 297−307.
(25) Allen, N. S.; Luengo, C.; Edge, M.; Wilkinson, A.; Parellada, M. D.; Barrio, J. A.; Santa, Quiteria, V. R. *J. Photochem. Photobiol. A* **2004**, *162*, 41−51.
(26) Thomas, M.; Richardson, H. H. *Vibr. Spectrosc.* **2000**, *24*, 137−146.
(27) Noda, I.; Dowrey, A. E.; Marcott, C.; Story, G. M.; Ozaki, Y. *Appl. Spectrosc.* **2000**, *54*, 236−248.
(28) Noda, I.; Ozaki, Y. *Two-dimensional Correlation Spectroscopy—Applications in Vibrational and Optical Spectroscopy*; John Wiley & Sons: Chichester, U.K., 2004.
(29) Wu, Y. Q.; Meersman, F.; Ozaki, Y. *Macromolecules* **2006**, *39*, 1182−1188.
(30) Noda, I. *Appl. Spectrosc.* **1993**, *47*, 1329−1336.
(31) Morita, S.; Shinzawa, H.; Tsenkova, R.; Noda, I.; Ozaki, Y. *J. Mol. Struct.* **2006**, *799*, 111−120.
(32) Shinzawa, H.; Morita, S.; Noda, I.; Ozaki, Y. *J. Mol. Struct.* **2006**, *799*, 28−33.
(33) Morita, S.; Shinzawa, H.; Noda, I.; Ozaki, Y. *J. Mol. Struct.* **2006**, *799*, 16−22.
(34) Sasic, S.; Katsumoto, Y.; Sato, N.; Ozaki, Y. *Anal. Chem.* **2003**, *75*, 4010−4018.
(35) Morita, S.; Shinzawa, H.; Noda, I.; Ozaki, Y. *Appl. Spectrosc.* **2006**, *60*, 398−406.
(36) Noda, I. *Appl. Spectrosc.* **2000**, *54*, 994−999.
(37) Krimm, S. *Adv. Polym. Sci.* **1960**, *2*, 51−172.
(38) Holland-Moritz, K.; Sausen, E. *J. Polym. Sci., Polym. Phys.* **1979**, *17*, 1−23.
(39) Ishioka, T.; Wakisaka, H.; Kanesaka, I.; Nishimura, M.; Fukasawa, H. *Polymer* **1997**, *38*, 2421−2430.
(40) Sharma, P.; Tandon, P.; Gupta, V. D. *Eur. Polym. J.* **2000**, *36*, 2629−2638.
(41) Naka, Y.; Nemoto, N.; Song, Y. *J. Polym. Sci., Polym. Phys.* **2005**, *43*, 1520−1531.
(42) Sworen, J. C.; Smith, J. A.; Berg, J. M.; Wagener, K. B. *J. Am. Chem. Soc.* **2004**, *126*, 11238−11246.
(43) Sasaki, T.; Tanaka, M.; Takahashi, T. *Polymer* **1997**, *38*, 4765−4768.
(44) Painter, P. C.; Koenig, J. L. *J. Polym. Sci., Polym. Phys.* **1977**, *15*, 1885−1903.
(45) Painter, P. C.; Kessler, R. E.; Snyder, R. W. *J. Polym. Sci., Polym. Phys.* **1980**, *18*, 723−729.
(46) Xue, G.; Wang, Y.; Gu, X.; Lu, Y. *Macromolecules* **1994**, *27*, 4016−4017.
(47) Painter, P.; Sobkowiak, M.; Park, Y. *Macromolecules* **2007**, *40*, 1730−1737.
(48) Jokela, K.; Vaananen, A.; Torkkeli, M.; Starck, P.; Serimaa, R.; Lofgren, B.; Seppala, J. *J. Polym. Sci., Polym. Phys.* **2001**, *39*, 1860−1875.
(49) Carella, J. M.; Graessley, W. W.; Fetters, L. J. *Macromolecules* **1984**, *17*, 2775−2786.
(50) Crist, B.; Claudio, E. S. *Macromolecules* **1999**, *32*, 8945−8951.
(51) Starck, P.; Rajanen, K.; Lofgren, B. *Thermochim. Acta* **2003**, *395*, 169−181.
(52) Rong, W. R.; Fan, Z. Y.; Yu, Y.; Bu, H. S.; Wang, M. *J. Polym. Sci., Polym. Phys.* **2005**, *43*, 2243−2251.
(53) Marti, E.; Kaisersberger, E.; Moukhina, E. *J. Therm. Anal. Calorim.* **2006**, *85*, 505−525.
(54) Modi, M. A.; Krishnamoorti, R.; Tse, M. F.; Wang, H. C. *Macromolecules* **1999**, *32*, 4088−4097.
(55) Krishnamoorti, R.; Silva, A. S.; Modi, M. A.; Hammouda, B. *Macromolecules* **2000**, *33*, 3803−3809.
(56) Krishnamoorti, R.; Modi, M. A.; Tse, M. F.; Wang, H. C. *Macromolecules* **2000**, *33*, 3810−3817.
(57) Hiki, Y.; Kogure, Y. *J. Non-Cryst. Solids* **2003**, *315*, 63−69.
(58) Hiki, Y.; Kosugi, T. *J. Non-Cryst. Solids* **2005**, *351*, 1300−1306.
(59) Dai, Q.; Lu, Y.; Xue, G.; Liao, Y. T. *Polym. Bull. (Berlin)* **1995**, *35*, 209−214.
(60) Watanabe, A.; Morita, S.; Ozaki, Y. *Biomacromolecules* **2006**, *7*, 3164−3170.
(61) Watanabe, A.; Morita, S.; Ozaki, Y. *Appl. Spectrosc.* **2006**, *60*, 611−618.

MA071630P